Up2010: Have Observations Revealed a Variable Upper End of the Initial Mass Function?
ASP Conference Series, Vol. 440
Marie Treyer, Ted K. Wyder, James D. Neill, Mark Seibert, and Janice C. Lee, eds.

Type IIn Supernova Detections in $z \sim 2$ Lyman Break Galaxies: Probing the IMF Directly

Jeff Cooke,[1] Mark Sullivan,[2] Elizabeth J. Barton,[3] Richard S. Ellis,[1] and Avishay Gal-Yam[4]

[1] *California Institute of Technology, 1200 E. California Blvd. Pasadena, CA 91125, USA*

[2] *Department of Physics, University of Oxford, Denys Wilkinson Building, Keble Road, Oxford, OX1 3RH, UK*

[3] *Department of Physics & Astronomy, Center for Cosmology, University of California, Irvine, Irvine, CA 92697, USA*

[4] *Benoziyo Center for Astrophysics, Weizmann Institute of Science, 76100 Rehovot, Israel*

Abstract. Type IIn supernovae (SNe IIn) exhibit luminous ultraviolet continua during outburst and luminous, long-lived narrow ultraviolet and optical emission lines attributed to circumstellar interaction. These properties have enabled successful detections at $z \sim 2$ in archival imaging and continued investigations from late-time spectroscopy. Because SNe IIn are believed to have massive ($\gtrsim 50 M_\odot$) progenitors, searches in the well-studied Lyman break galaxy (LBG) host population offer the prospect of testing the form of the high-redshift stellar initial mass function (IMF) in a high density star formation environment directly. I briefly discuss our $z \sim 2$ photometric detection method targeting LBGs in the Canada-France-Hawaii Telescope Legacy Survey (CFHTLS) and present data from the first 6 confirmed $z \sim 2$ SNe IIn pulled from 30 photometric SN candidates. A comparison of the color and magnitude distributions of the SN host galaxies to that of the full LBG sample finds that $z \sim 2$ SNe preferentially occur in bluer, fainter galaxies. I conclude with a discussion of an approach that uses the CFHTLS pilot sample to provide a first estimate of the form of the high-redshift IMF. Upcoming deep synoptic imaging surveys will greatly improve $z \sim 2$ SNe IIn statistics from $\sim 10^5$ expected detections and future large aperture space- and ground-based telescopes will have the sensitivities to extend this work to $z \gtrsim 6$.

1. Introduction

Supernovae (SNe) that are intrinsically luminous in the restframe ultraviolet (UV) are excellent candidates for high-redshift detection in deep, wide-field optical surveys. To date, type IIn supernovae (SNe IIn; Schlegel 1990) and rare hyper-luminous SNe have been shown to have high UV luminosities and photometric and/or spectroscopic features that enable their detection and classification at $z = 1 - 2$ in existing data (Cooke 2008; Cooke et al. 2009; Quimby et al. 2009). Moreover, a growing body of evidence supports a picture where these SN types have very massive progenitors ($\gtrsim 50 M_\odot$; Gal-

Yam et al. 2007; Gal-Yam & Leonard 2009; Gal-Yam et al. 2009; Smith et al. 2007, 2010a,b) and, as a result, the form of the stellar initial mass function (IMF) has a direct and measurable effect on the expected number of these events. Consequently, low to high redshift detection in well-defined galaxy samples offer the tantalizing possibility to probe the form of the IMF in differing star-formation density environments over a large span of cosmic time.

In Cooke et al. (2009), we present evidence for the detection and spectroscopic confirmation of the first two SNe IIn at $z \sim 2$ followed up from a complete list of photometric candidates detected in the four square-degree fields of the Deep component of the Canada-France-Hawaii Telescope Legacy Survey (CFHTLS). At this conference, I report on the confirmation of four additional $z \sim 2$ events and briefly discuss the properties of the high redshift SN host galaxies. Finally, I discuss an approach that uses the CFHTLS sample to place a first constraint on the form of the high-redshift IMF and the suggested implications of the data acquired to date.

2. Photometric Detection

All photometric observations utilize the high-quality images of the Deep component of the CFHTLS during the 2003 through 2007 seasons (see Cooke et al. 2009, , Supplementary Information for a description). The observing strategy of the CFHTLS produced $g'r'i'$-band images of each field at a regular cadence over $\sim 25-30$ nights per $5-6$ month observing season. Imaging in the u^* and z'-bands to similar depths were also obtained, but not necessarily at the same cadence as the $g'r'i'$-bands. Only images with seeing FWHM < 0.75 arcsec are combined to create high-quality stacked images. High-redshift host galaxies are color selected using the Lyman break technique (Steidel et al. 1996, 1999) in deep four-year $u^*g'r'i'z'$ "super stack" images and SN events are searched for in yearly $g'r'i'$ "seasonal stack" images (limiting magnitude of $r \sim 26.5$). We flag galaxies that meet $z \sim 2$ and $z \sim 3$ $u^*g'r'i'z'$ color-selection criteria and monitor the flux of these Lyman break galaxies (LBGs) in the "seasonal stacks" over four CFHTLS seasons.

In this work we focus on $z \sim 2$ because after analyzing the CFHT MegaCam $u^*g'r'i'z'$ filter set, the depth of the stacked images, and ~ 200 Keck spectra obtained specifically for this program, we find that LBG selection at $z \sim 2$ is the lowest redshift that provides the highest efficiency for spectroscopic follow up and that $z \sim 2$ is the highest redshift that a statistical sample of SNe IIn are expected to be detected at the given depths of the CFHTLS "seasonal stack" images.

As a result of time dilation, SNe IIn at $z \sim 2$ are expected to be detectable for $\sim 3-6$ months at the sensitivity of the "seasonal stack" images. Because the observing seasons are separated by $6-7$ months, $z \sim 2$ SN are expected to only significantly contribute to a single "seasonal stack" image. Monitored LBGs that exhibit flux increases in only one season and meet SN detection criteria described in Cooke et al. (2009, 2011) are considered SN candidate hosts and slated for follow-up spectroscopy. We find 30 events that qualify as $z \sim 2$ SN candidates in the four square-degree fields over the two central seasons. Although AGN can mimic the photometric behavior of SNe, we find that in principle all, or nearly all, AGN can be removed by examining their $g'r'i'$ light curve behavior (Figure 1). Spectroscopic follow-up on a sample of six of the "SN-like" AGN candidates shows this analysis to be highly efficient, as all six are identified as AGN.

3. Spectroscopic Confirmation

The spectroscopic data for this program were obtained using the Low Resolution Imaging Spectrograph (LRIS, Oke et al. 1995; McCarthy et al. 1998) and the DEep Imaging Multi-Object Spectrometer (DEIMOS, Faber et al. 2003) on the Keck Telescopes. These instruments were used in multi-object mode to acquire deep spectra of the supernovae and of ~ 300 $z \sim 2$ and $z \sim 3$ LBGs to test our host galaxy photometric color selection criteria and help refine the properties and volume of the monitored host galaxies.

To date, six of the 30 photometric $z \sim 2$ SN candidates received follow-up deep spectroscopy. All six SNe are confirmed to reside in host LBGs with $2.0 < z < 2.4$ and display evidence of restframe UV emission lines that are observed locally at similar times after explosion (Fransson et al. 2002, 2005) and are thus classified as SNe IIn. Two of the six spectra are shown in Figure 2. The Lyα emission feature of LBGs is observed to be redshifted by $\sim 450 \pm 300$ km s^{-1} from the systemic velocity (Adelberger et al. 2003; Shapley et al. 2003; Cooke et al. 2005) and is attributed to the escape of off-resonance photons scattered off of the receding portion of outflowing material driven by galactic-scale superwinds. In contrast, the peaks of the emission lines in local SNe IIn have been observed to be blueshifted by $\sim 1000 - 4000$ km s^{-1} (e.g., Filippenko 1997; Leonard et al. 2000; Fransson et al. 2002, 2005). These features work to help separate SN Lyα emission from host galaxy Lyα emission (Figure 2). SN IIn UV emission features also include shock-ionization transitions, such as N IV and N III and have C IV/C III ratios that are not observed in LBG or AGN spectra (see Cooke et al. 2009, Supplementary Information for more details). However, the SN UV emission features redward of Lyα are susceptible to dilution by similar, and strong, host galaxy UV absorption features and can appear less prominent in the spectra.

4. Host Galaxies

The redshifts of the six confirmed SNe are representative of the redshift path probed by the monitored LBGs ($z = 2.2 \pm 0.3$). We compare the r' magnitude and $(g' - i')$ color distributions of our full LBG sample with those for host galaxies of the 30 SN candidates and 6 confirmed events. As can be seen in Figure 3, SNe IIn at $z \sim 2$ appear to prefer overall fainter and bluer LBG hosts when compared to the respective medians of the full sample.

We analyzed the "seasonal stacks" for all four observing seasons but selected SN candidates from the central two seasons only (2004-2005 and 2005-2006). This assures that the single season flux increase from potential SN events begins and returns to the nominal host galaxy flux level in the non-detection seasons.

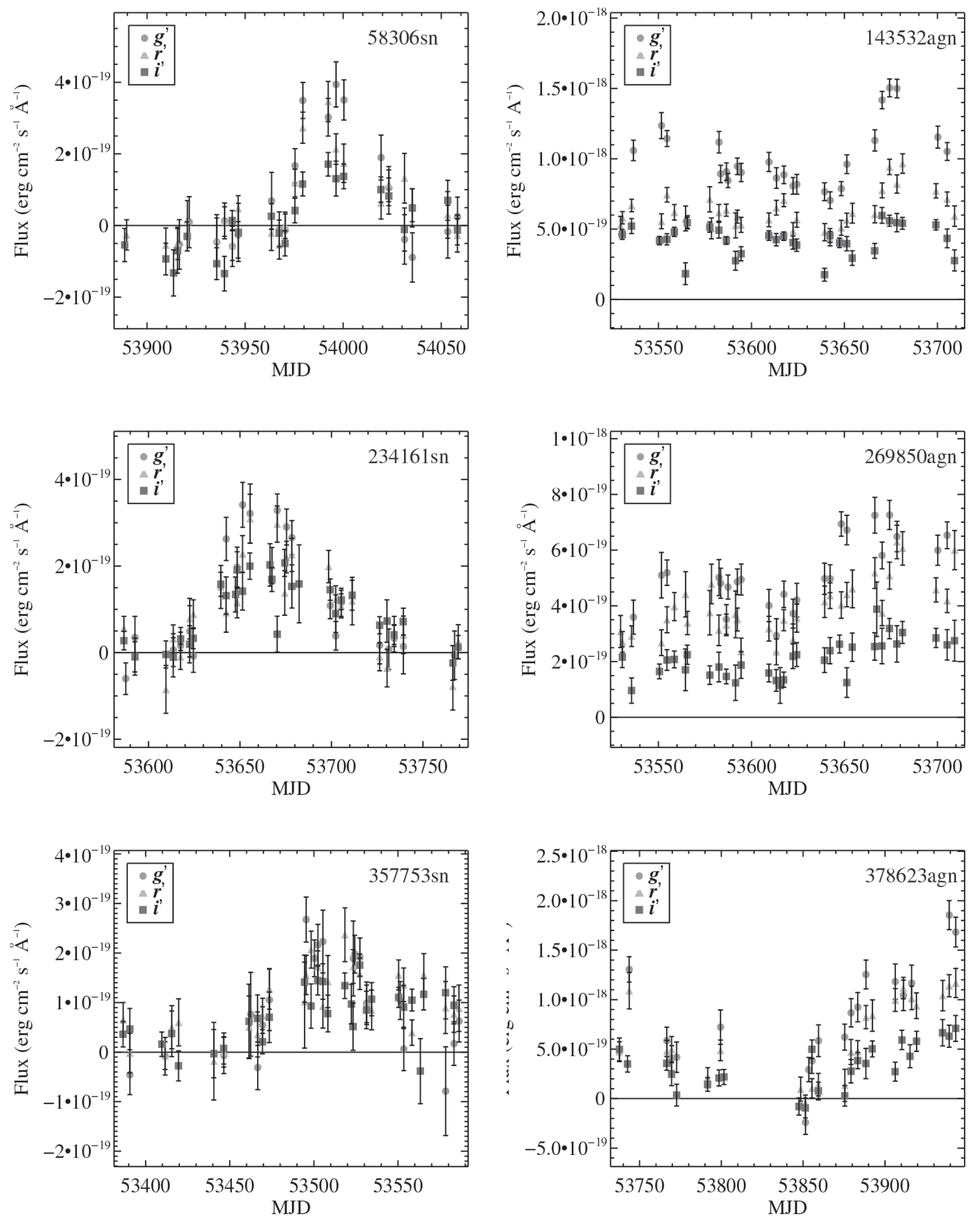

Figure 1. CFHTLS $g'r'i'$-band light curves for three $z \sim 2$ SN IIn and three $z \sim 2$ AGN. The stable host galaxy flux during all adjacent seasons and single, well-sampled smooth light curve rise and decay during the detection season help separate SN events *(left column)* from AGN flux variations *(right column)* which are observed to be erratic with multiple variations well above the average flux of the host (set to zero in the plots).

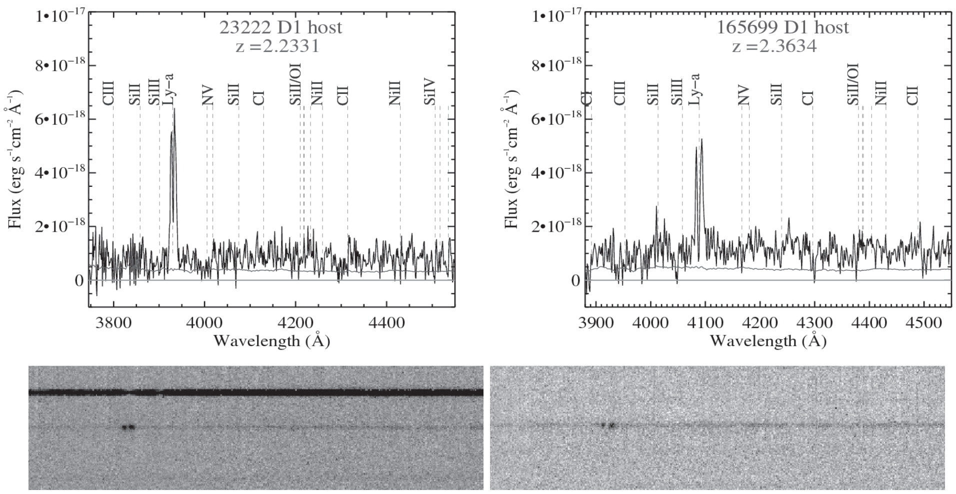

Figure 2. Spectra of two $z \sim 2$ SNe located in the CFHTLS 'D1' field (SN 23222 *left* and SN 165699 *right*). **Upper two panels:** The vertical dashed lines mark the locations of expected strong ISM features that are used help to identify $z \sim 2$ LBGs. The SNe display blueshifted UV emission features similar to those seen in low-redshift SN IIn spectra, including strong Lyα emission. **Lower two panels:** Two-dimensional spectra corresponding to the one-dimensional spectra directly above each panel and covering approximately the same wavelength range. The small offsets of the SN and host LBG Lyα emission in the spatial direction are consistent with the offsets of the SN and host LBG flux centroids in the images measured at the position angles of the spectroscopy. Although $\sim$ 50% of $z \sim 2$ LBGs exhibit dominant Lyα in emission (typically redshifted with respect to systemic; see text), we find that all $z \sim 2$ SN confirmations to date reside in LBGs with this feature.

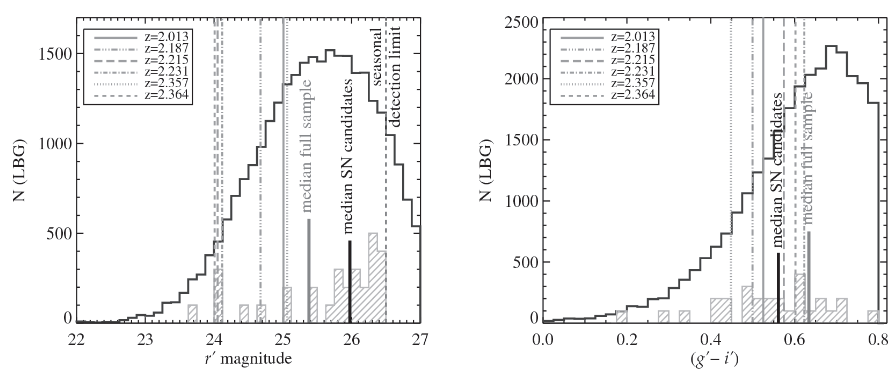

Figure 3. Histograms of r' mag and $(g' - i')$ color of the monitored $z \sim 2$ LBGs. The full LBG sample is indicated by the empty histograms whereas the SN candidate hosts are shown as the hatched histogram ($\times 100$ to be more visible in the plot). Full-length vertical lines denote the respective values for the spectroscopically confirmed $z \sim 2$ SN hosts and are labeled in the legend. Half-length solid vertical lines denote the median values of the full (gray) and SN host (black) samples as indicated.

Interestingly, we find that every SN host LBG displays dominant Lyα in emission. This feature may lend insight into the environments and star formation histories of the SN hosts. For example, Cooke et al. (2010) report a strong relationship between Lyα emission and pair separation in $z \sim 3$ LBGs. We find that every LBG residing in a spectroscopic close pair ($<$ 20 kpc, physical) and every spectroscopic LBG with a photometric close companion exhibits dominant Lyα in emission, with a decrease in the fraction of LBGs exhibiting dominant Lyα in emission with increased separations. Because only $\sim$ 50% of the LBG population exhibits dominant Lyα in emission, the presence of this spectroscopic feature may help to indicate a recent interaction or merger. These processes can trigger new star formation, therfore, observing galaxies during these stages of evolution may play a role in enabling the detection of the deaths of very massive stars.

5. Implications on the IMF

LBGs at $z \sim 2-3$ have high average star formation rates ($\sim 30-40 M_\odot$ yr^{-1}; e.g., Shapley et al. 2003; Erb et al. 2006), and therefore probe star formation environments similar to those of local starburst galaxies. We monitor a finite number of LBGs over a well-defined volume and use star formation rates derived from the observed UV flux. As a result, we can compute the *relative* number of $z \sim 2$ SNe IIn in the CFHTLS for various adopted forms of the IMF. This is because the relative number of detectable SNe IIn is largely unaffected by dust because the underlying star formation rate, based on the escaping UV flux, counters the amount of extinction (Dahlén & Fransson 1999).

The total expected number of detectable SNe IIn using this approach depends on many factors, which include the sensitivity of each CFHTLS "seasonal stack" image to detect SN events in LBGs as a function of host galaxy magnitude, the star formation rates specific to the galaxies in our sample, the volume probed by the LBG color selection method, and the SN IIn UV luminosity distribution and progenitor mass range. Many of these parameters have been accurately determined for the CFHTLS directly or by Monte Carlo analysis and LBG spectroscopic follow-up. Although good observational and theoretical progress has been made on the latter two parameters, they maintain the largest uncertainties. Nevertheless, because top-heavy IMF models used to reconcile independent low and high redshift observations (e.g., Davé 2008; Chary 2008) predict a factor of ~ 3 *greater* number of SNe IIn compared to local expectations ($\alpha \sim -2.35$), such a difference is detectable with the CFHTLS sample within reasonable estimates of the above uncertainties.

Using the values determined for the images and local estimates for the SN IIn parameters, we compute an expected 8.3 ± 1.9 SNe IIn for the four fields over the two central seasons of the CFHTLS using a Salpeter IMF ($\alpha = -2.35$) and 26.4 ± 6.2 for a top heavy IMF ($\alpha = -1.6$), where the error is the field-to-field expectation scatter. Interestingly, we find 30 SN candidates and have confirmed six. At this early stage, and considering the caveats, the data can only provide a suggestion that the high-mass end slope of the $z \sim 2$ IMF is $\alpha \sim -2.4$ and that the slope will move towards $\alpha \sim -1.4$ with each future SN confirmation. An illustration of this concept is shown in Figure 4.

The upcoming Hyper-SuprimeCam and the Large Synoptic Survey Telescope surveys are expected to detect $\sim 40,000$ SNe IIn at $z \sim 2$ over 10 years and completely characterize the high-redshift population. Once the UV magnitude distribution and

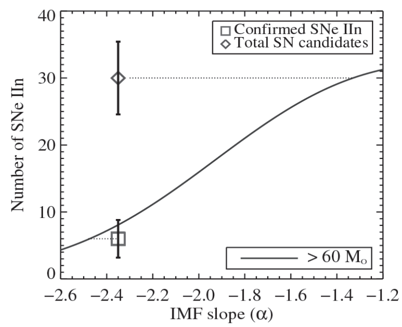

Figure 4. Illustration of the concept of using SN counts to constrain the form of the IMF. The curve represents the number of SNe IIn as a function of IMF slope, α, expected for the program discussed here assuming a progenitor mass of $\geq 60 M_{\odot}$ (see text). The six SNe IIn confirmed to date (square) and 30 SN candidates (diamond) detected in the CFHTLS are placed at $\alpha = -2.35$ arbitrarily. The horizontal dotted lines indicate the central value of the slope implied by the confirmed SNe IIn to date ($\alpha \sim -2.47$) and if all 30 SN candidates are confirmed ($\alpha \sim -1.35$). Our pilot program with the CFHTLS aims to secure redshift for all 30 candidates and place the first estimate of the IMF slope at $z \sim 2$.

progenitor mass range of SNe IIn are refined, SN IIn counts can offer a new avenue to measure the slope of the IMF at high-redshift using direct means. Moreover, the deep component of Hyper-SuprimeCam will have the capability to extend SN IIn detections to $z \sim 6$. Finally, future 30m-class telescopes and the James Webb Space Telescope, will have the sensitivities to spectroscopically confirm and study high redshift SNe IIn in detail and probe the IMF to the epoch of reionization.

Acknowledgments. Based on observations obtained with MegaPrime/MegaCam, a joint project of CFHT and CEA/DAPNIA, at the Canada-France-Hawaii Telescope (CFHT) which is operated by the National Research Council (NRC) of Canada, the Institut National des Science de l'Univers of the Centre National de la Recherche Scientifique (CNRS) of France, and the University of Hawaii. This work is based in part on data products produced at the Canadian Astronomy Data Centre as part of the Canada-France-Hawaii Telescope Legacy Survey, a collaborative project of NRC and CNRS.

References

Adelberger, K. L., Steidel, C. C., Shapley, A. E., & Pettini, M. 2003, ApJ, 584, 45
Chary, R. 2008, ApJ, 680, 32
Cooke, J. 2008, ApJ, 677, 137
Cooke, J., Barton, E. J., Sullivan, M., Bullock, J. S., Carlberg, R. G., Gal-Yam, A., & Tollerud, E. 2009, Nat, 460, 237
Cooke, J., Berrier, J. C., Barton, E. J., Bullock, J. S., & Wolfe, A. M. 2010, MNRAS, 403, 1020
Cooke, J., Sullivan, M., Barton, E. J., Ellis, R. S., Bullock, J. S., Gal-Yam, A., Tollerud, E., & Newman, A. 2011, in preparation
Cooke, J., Wolfe, A. M., Prochaska, J. X., & Gawiser, E. 2005, ApJ, 621, 596
Dahlén, T., & Fransson, C. 1999, A&A, 350, 349
Davé, R. 2008, MNRAS, 385, 147

Erb, D. K., Steidel, C. C., Shapley, A. E., Pettini, M., Reddy, N. A., & Adelberger, K. L. 2006, ApJ, 647, 128

Faber, S. M., Phillips, A. C., Kibrick, R. I., Alcott, B., Allen, S. L., Burrous, J., Cantrall, T., et al. 2003, in Society of Photo-Optical Instrumentation Engineers (SPIE) Conference Series, edited by M. Iye & A. F. M. Moorwood, vol. 4841 of Presented at the Society of Photo-Optical Instrumentation Engineers (SPIE) Conference, 1657

Filippenko, A. V. 1997, ARA&A, 35, 309

Fransson, C., Challis, P. M., Chevalier, R. A., Filippenko, A. V., Kirshner, R. P., Kozma, C., Leonard, D. C., et al. 2005, ApJ, 622, 991

Fransson, C., Chevalier, R. A., Filippenko, A. V., Leibundgut, B., Barth, A. J., Fesen, R. A., Kirshner, R. P., et al. 2002, ApJ, 572, 350

Gal-Yam, A., & Leonard, D. C. 2009, Nat, 458, 865

Gal-Yam, A., Leonard, D. C., Fox, D. B., Cenko, S. B., Soderberg, A. M., Moon, D., Sand, D. J., et al. 2007, ApJ, 656, 372

Gal-Yam, A., Mazzali, P., Ofek, E. O., Nugent, P. E., Kulkarni, S. R., Kasliwal, M. M., Quimby, R. M., et al. 2009, Nat, 462, 624

Leonard, D. C., Filippenko, A. V., Barth, A. J., & Matheson, T. 2000, ApJ, 536, 239

McCarthy, J. K., Cohen, J. G., Butcher, B., Cromer, J., Croner, E., Douglas, W. R., Goeden, R. M., et al. 1998, in Society of Photo-Optical Instrumentation Engineers (SPIE) Conference Series, edited by S. D'Odorico, vol. 3355 of Presented at the Society of Photo-Optical Instrumentation Engineers (SPIE) Conference, 81

Oke, J. B., Cohen, J. G., Carr, M., Cromer, J., Dingizian, A., Harris, F. H., Labrecque, S., et al. 1995, PASP, 107, 375

Quimby, R. M., Kulkarni, S. R., Kasliwal, M. M., Gal-Yam, A., Arcavi, I., Sullivan, M., Nugent, P., et al. 2009, ArXiv e-prints. `astro-ph/0910.0059`

Schlegel, E. M. 1990, MNRAS, 244, 269

Shapley, A. E., Steidel, C. C., Pettini, M., & Adelberger, K. L. 2003, ApJ, 588, 65

Smith, N., Chornock, R., Silverman, J. M., Filippenko, A. V., & Foley, R. J. 2010a, ApJ, 709, 856

Smith, N., Li, W., Filippenko, A. V., & Chornock, R. 2010b, ArXiv e-prints. `astro-ph/1006.3899`

Smith, N., Li, W., Foley, R. J., Wheeler, J. C., Pooley, D., Chornock, R., Filippenko, A. V., et al. 2007, ApJ, 666, 1116

Steidel, C. C., Adelberger, K. L., Giavalisco, M., Dickinson, M., & Pettini, M. 1999, ApJ, 519, 1

Steidel, C. C., Giavalisco, M., Pettini, M., Dickinson, M., & Adelberger, K. L. 1996, ApJ, 462, L17+